nzsee
NEW ZEALAND SOCIETY FOR EARTHQUAKE ENGINEERING

Seismic ratcheting considerations

M. H. Baloch, G. A. MacRae & C-L. Lee
Department of Civil and Natural Resources Engineering, University of Canterbury, Christchurch, New Zealand.

ABSTRACT

This paper uses time history analysis to quantify effects of ratcheting on single storey structures. The ratcheting tendency was characterized by static axial forces on a horizontal single degree of freedom (SDOF) spring model. This represented a cantilever structure subjected to initial gravity forces and the hysteresis loop is assumed to account for *P*-delta effects. The structures had flag shaped hysteresis loops with different amounts of hysteretic energy dissipation. Loop behaviour ranged from bilinear elastic with no post-elastic stiffness to elastoplastic. Different structural periods, strengths and ground motion records were considered.

It is shown that as the strength difference in the forward and reverse directions increased, the tendency for increased seismic displacements in one direction increased. Ratcheting of the model with greater hysteretic energy dissipation was significantly greater than that of the models with more pinched loops. The relationships obtained were consistent with those found previously for both steel and reinforced concrete structures as proposed for the part 5 of New Zealand Structural Design Actions standard, NZS 1170.5:2004, but significantly more information was obtained because of a wider range of hysteresis loop and structural period was investigated. From the results obtained, simple recommendations are provided for use in structural design.

1 INTRODUCTION

Seismic ratcheting refers to the phenomena by which structures predominately deform more in one direction compared to the other during an earthquake event. Ratcheting can occur due to (i) the ground motion characteristics, (ii) *P*-delta effects, (iii) hysteretic effects, (iv) eccentric gravity loading, and/or (v) strength/stiffness differences in different horizontal directions. Structural displacement demands are more likely to be underestimated when the possibility of seismic ratcheting design is not considered (MacRae et al., 2022). It can result in unexpected deformations, damage, or possible structural collapse (Yeow and Kusunoki, 2023). This work considers ratcheting due to different lateral force resistance in opposite horizontal directions. This can occur due to an applied eccentric gravity loading, and/or structural properties.

One example of seismic ratcheting, reported by the Canterbury Earthquake Royal Commission (Cooper et al., 2012), involved the Christchurch Hotel Grand Chancellor (HGC) during the 22 February 2011 earthquake. This structure had a cantilevered portion on its east bay over an existing lane as shown in Figure 1a. This imposed an eccentric gravity moment on the structure as shown in Figure 1b. It may be seen that analyses indicate greater displacements toward the east due to ratcheting in Figure 1c. The design for this structure had used the modal response spectrum analysis (RSA) method, which is based

on elastic analysis, so it does not consider the lateral strength resistance difference in both the forward and reverse directions on the inelastic response which leads to ratcheting (Yeow and Kusunoki, 2023).

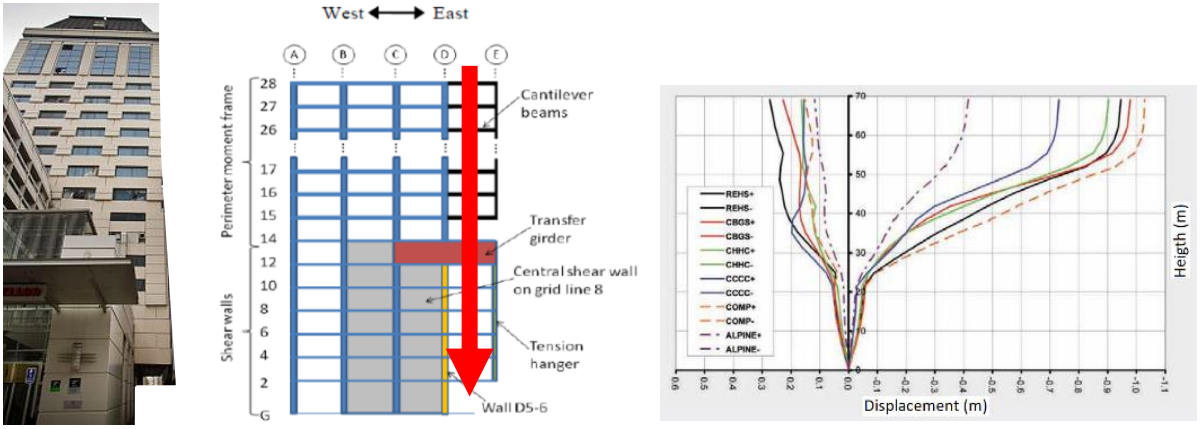

(a) Building *(b) Eccentric Force* *(c) Peak displacements from time history analyses*

Figure 1: Hotel Grand Chancellor (Cooper et al., 2012)

While some structures have significant ratcheting tendencies due to strength/stiffness differences in opposite horizontal directions, or due to eccentric gravity loading, ordinary regular structures may have these effects to some extent too due to movement of live load within the structure, or differences in the properties of members which are nominally the same. Therefore, structures are not binary, with or without a ratcheting tendency, so it is the degree of ratcheting tendency that is important.

Numerous investigations have been conducted to quantify the amplification of displacements in structures due to ratcheting, and some of these have resulted in modifications to standards, as well as in publications. However, in general the shapes of the hysteresis loops considered have been limited making it difficult for engineers to understand the likely ratcheting effects for general structures.

For engineers to conduct design of structures with confidence, often using elastic analyses in their design methods, there is a need for guidance to consider the possibility of ratcheting.

This work aims to address this requirement by exploring the answers to the following questions:

1) How do different structural properties affect the ratcheting tendency?
2) How good are the NZS1170.5 provisions, and proposed provisions for seismic ratcheting?
3) Can simple design guidance be developed from the work conducted?

2 PREVIOUS WORK

The Japan Road Association (JRA 1990) for bridge column was among the first to recognise and consider ratcheting. It explained that eccentric gravity loading can cause a moment at the base of a column by an amount equal to the eccentric vertical load multiplied by the eccentricity. It suggests the provision of an additional flexural strength that should be equal to the applied eccentric moment (M_E) to counter the ratcheting effects (MacRae et al., 2022). However, MacRae and Kawashima (1993) explained the ratcheting tendency of a structure by defining hysteresis dynamic stability and using a concept called the *hysteresis centre curve* (HCC). The additional flexural strength required to be provided in the direction of the eccentric moment for minimising the ratcheting effects in a bridge column exhibiting elastic perfectly plastic (EPP) behaviour was found to be $2M_E$. This was also endorsed by Yeow et al., (2013) when inelastic time history analyses were conducted on a cantilever column using a suite of earthquake records to estimate the strength required for minimizing the ratcheting-related displacement response. The strength difference was quantified using the strength difference ratio (β) described in Equation 1, where M^+ was defined as the moment capacity in the stronger direction while M^- was the moment capacity in the weaker direction and M_E was the applied

eccentric moment. Additionally, it was observed that the additional strength requirement for mitigating the ratcheting effects in structures having Takeda hysteric behaviour can be higher than that having EPP behaviour. An additional flexural strength of 2.3M_E was recommended for structures exhibiting Takeda hysteretic loops.

$$B = \frac{M^+ - M^-}{M_E} \quad (1)$$

Canadian seismic codes (NBCC, 2015) incorporated the recommendations from Dupuis et al., (2014) to tackle the gravity-induced lateral demands on seismic force resisting system. The recommendations were made based on the results of the analysis of a symmetric structure with eccentric moments. These ratcheting recommendations, given in Table 1, suggest the amplification of the displacement demands based on the ratio of imposed eccentric moment to the yield capacity of the member in the direction of the eccentric moment, α.

Table 1: Canadian Ratcheting Provisions (Dupuis et al., 2014)

Systems with self-centring characteristics	**Other systems**	**Requirements**
$0.0 \leq \alpha \leq 0.1$	$0.0 \leq \alpha \leq 0.03$	No requirements
$0.1 < \alpha \leq 0.2$	$0.03 < \alpha \leq 0.06$	Multiply displacements by 1.2
$0.2 < \alpha$	$0.06 < \alpha$	Non-Linear response history analysis

Seismic ratcheting provisions were included in the 2016 amendment to the New Zealand structural design actions standard (NZS1170.5, 2016). They were based on a total of 1500 time history analyses of a single degree of freedom structures with periods ranging from 0.5s to 2.5s, lateral force reduction factors from 1 to 5, using the Takeda hysteretic model for the plastic hinges. *P*-delta effects and the stiffness and strength interaction of reinforced concrete was also ignored for these analyses (Saif 2017). A ratcheting index, r_i, is used to evaluate the ratcheting tendency which is found using Equation 2. In Equation 2, $r_{i,1}$ accounts for lateral strength differences in two opposite directions according to Equation 3, while $r_{i,2}$ considers any changes made in the lateral strength for balancing the eccentric gravity load effects in Equation 4.

$$r_i = r_{i,1} + r_{i,2} \quad (2)$$

$$r_{i,1} = \frac{lateral\ strength\ in\ forward\ direction,\ S_f}{lateral\ strength\ in\ reverse\ direction,\ S_r} \quad (3)$$

$$r_{i,2} = \frac{change\ in\ strength\ in\ forward\ direction,\ S_g}{lateral\ strength\ in\ reverse\ direction,\ S_r} \quad (4)$$

Table 2 from NZS 1170.5 (2016) indicates that ratcheting does not need to be explicitly considered when r_i is less than 1.15. Also, for larger ratcheting tendencies (r_I > 1.5), more advanced analysis is required.

Table 2: NZS1170.5 (2016) provisions for ratcheting consideration (Standards New Zealand 2016)

Ratcheting index (r_i)	**Requirement**
$r_i < 1.15$	Influence of seismic ratcheting can be ignored
$1.15 < r_i \leq 1.5$	Deflections modified by $0.75r_i+0.25$
$r_i > 1.5$	Non-linear dynamic analyses required

The NZS 1170.5 (2016) requirements were studied by Saif (2017) and Saif et al., (2017, 2018, 2022). Following the findings of numerical analysis carried out for steel and reinforced concrete (RC) columns carrying eccentric gravity loads and modelled as fibre sections, it was argued that the recommendations were reasonable for reinforced concrete structure displacement increase prediction, while non-conservative for steel structures. Also, the 2016 provisions were difficult to understand and apply. Modified requirements for seismic ratcheting were proposed (i) ignoring the second term in Equation 2, $r_{i,2}$, for computation of r_i, and (ii) considering also the behaviour of elastoplastic structures. These were included in the draft NZS 1170.5 proposed for 2019, but this document was not published. These are given in Table 3 (MacRae et al., 2022, and Yeow and Kusunoki, 2023). For the sake of clarity, the requirements in Table 2 and Table 3 are referred to as NZS1170.5 (2016) and NZS1170.5 (2019), respectively, for the remainder of this paper.

Table 3. NZS1170.5 (2019) proposed provisions for ratcheting consideration (MacRae et al., 2022)

Hysteretic behaviour	**Requirement**
Elastoplastic ($1.03 < r_i < 1.5$)	Deflections to be modified by $4r_i$-3
Pinched ($1.15 < r_i \leq 1.5$)	Deflections to be modified by $0.8r_i+0.2$

3 METHODOLOGY

A one-dimensional single-degree-of-freedom spring modelled as a zero-length element in OpenSEES, as shown in Figure 2a, was considered. A constant static force, P, causes the structure to have a force and displacement before the shaking starts. This spring model can relate to a cantilever column having an eccentric moment, M_E (= $P'e$), without the P-delta effect as shown in Figure 2b. Here, the equivalent lateral force on the structure is M_E/L, where L is the height of the column. The force P causes the structure to move the initial static displacement, Δ_s. The baseline about which oscillation occurs is shown by the red dashed line in Figure 2c. It may be seen that the structure will tend to yield in the negative direction rather than the positive direction, because the distance to the yield strength in the negative direction is lower than that in the positive direction. It will therefore tend to ratchet and have larger displacements in the negative direction.

The spring initial linear stiffness, K_i, for a given structural period, T, is found assuming a mass, m, for the oscillator using Equation 5. Furthermore, the model yield strength, F_y, was defined using Equation 6, where S_a is the spectral acceleration for the specified period of a given earthquake record, g is the acceleration due to gravity and R (Note: $R = k_\mu/S_p$ in NZS1170.5) is the lateral force reduction factor.

$$K_i = \frac{(2\pi)^2 * m}{T^2} \tag{5}$$

$$F_y = \frac{S_a * m * g}{R} \tag{6}$$

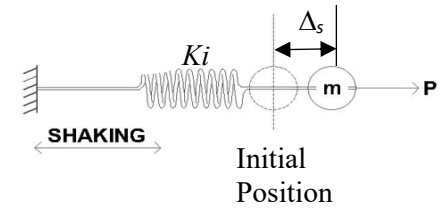

(a) Simple spring model used

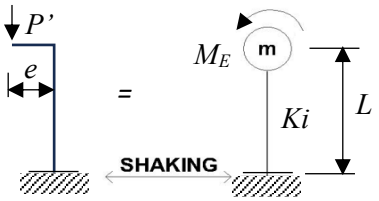

(b) Equivalent cantilever column

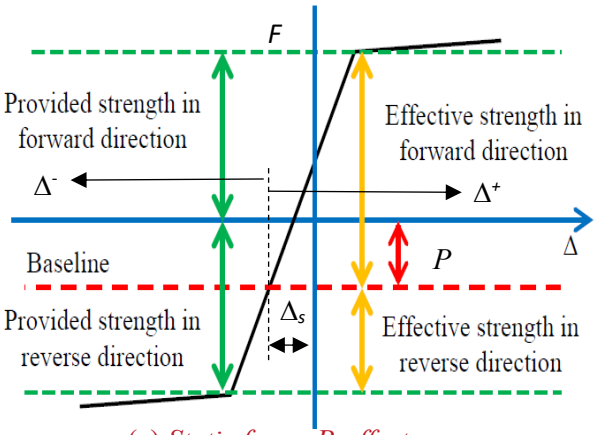

(c) Static force, P, effect

Figure 2. Structural Modelling

Analyses were carried out with r_i of 1.0, 1.02, 1.10, 1.30, 1.50 and 1.70 to compare with NZS1170.5 (2016 and 2019). Furthermore, to obtain the desired r_i, a static axial force, P, is applied to the model. The relation between r_i and P is given in Equation 7 because the positive direction strength increases by P, while that in the negative direction decreases by P as shown in Figure 2c. Therefore, the force P was found for a particular r_i and F_y using Equation 8.

$$r_i = \frac{F_y + P}{F_y - P} \tag{7}$$

$$P = F_y \times \frac{(r_i - 1)}{(r_i + 1)} \tag{8}$$

The flag-shaped hysteresis curve shown in Figure 3 has been used to model the hysteretic behaviour of the oscillator. The range of β has been used with the post elastic stiffness ratio (r) always being zero. When the flag-shaped hysteresis curve is used with β as 1 and r as zero, it will yield an EPP behaviour. Furthermore, damping was modelled using the bell-shaped damping model. The bell-shaped damping model developed by Lee (2020) allows user to define a constant damping ratio over a range of structural frequencies. Five different types of the said model have already been proposed that provide different possibilities for achieving a desired damping ratio curve. Type 0 is recommended when a uniform damping ratio is required within a positive range of frequency. The damping ratio selected is 5%. Damping is made proportional to the tangent stiffness. The damping model also provides the user with the choice of initial stiffness and converged stiffness variants which consider the initial stiffness and the current stiffness at the last converged time step to form the damping coefficient matrix respectively (Lee 2019, 2020, 2021, 2022; Lee and Chang 2023).

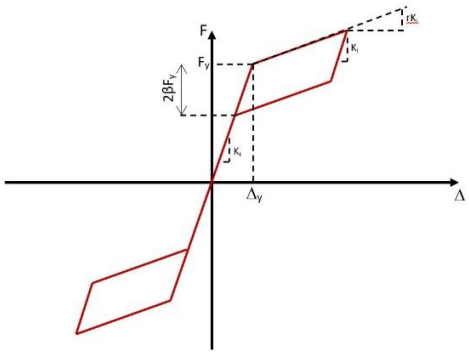

Figure 3. Flag-shape hysteresis curve

The far-field ground motion record suite from Appendix A of FEMA P695 was chosen for the analysis. It consists of 22 pairs of ground motions. Only horizontal components were utilized. FEMA P695 provides far-field and near-field record sets for nonlinear dynamic analysis. It recommends the use of Far-Field record set due to the unresolved issues related to the characterization and effects of Near-Field ground motion records (FEMA P695 2009). Each ground motion record has been applied twice, once in the forward direction and once in the reverse direction, to eliminate ratcheting arising due to the characteristics of the ground motion. Inelastic time history analysis was conducted with the Newmark-β method using $\alpha = 0.5$ and this $\beta = 0.25$, and an integration timestep always less than the period, $T/20$.

The model ratcheting is quantified in terms of the absolute maximum displacement ratio (AMDR) from Yeow and Kusunoki, (2023). In Equation 9, $\max|\triangle_{\text{ecc,dir1}}|$ and $\max|\triangle_{ecc,dir2}|$ are the absolute maximum displacement responses measured from the point where it has the static displacement Δ_s for the record applied in direction 1, and then in the opposite direction (i.e. direction 2), respectively, as shown in Figure 2c. The absolute maximum displacement of the model with a concentric static gravity force *P'* is $|\triangle_{con}|$ as shown in 2b. In this case, the eccentricity of *P'* is given by *e*, which is 0 so the column has no moment, M_E. This is modelled in Figure 2a using *P* of 0.0.

$$\text{AMDR} = \frac{max|\triangle_{ecc,dir1}|+max|\triangle_{ecc,dir2}|}{2|\triangle_{con}|} \tag{9}$$

The average absolute maximum displacement ratio (AAMDR) was calculated as the average value for the N_{rec} records using Equation 10, where the number of records, N_{rec}, is 22.

$$\text{AAMDR} = \frac{sum\ of\ AMDR}{Nrec} \tag{10}$$

The complete analysis scheme is shown graphical in Figure 4.

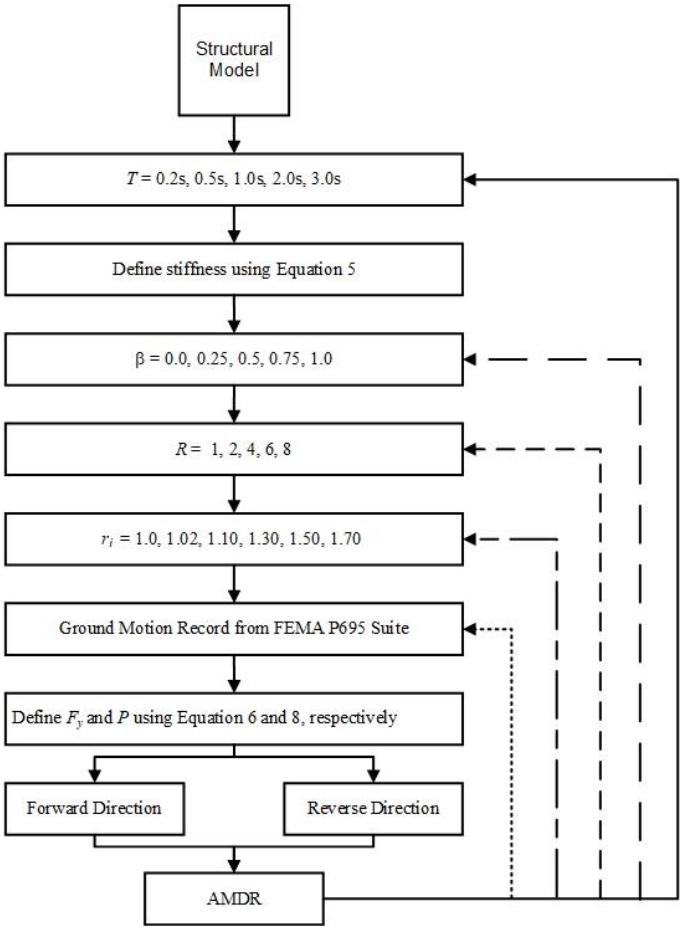

Figure 4. Analysis scheme

4 RESULTS AND DISCUSSION

4.1 Dynamic Response of Oscillators

Figures 5, 6, 7, 8 and 9 present the dynamic response of the oscillators for β of 1, 0.75, 0.5, 0.25 and 0, respectively, in terms of the average absolute maximum displacement ratio, AAMDR, for different periods with different lateral force reduction factor, *R*, values. In these graphs: NZSEP represents the NZS1170.5 (2016) recommendations for all structural types according to Table 2 which was based on analyses to represent reinforced concrete behaviour; NZSE represents the NZS1170.5 (2019) elastoplastic behaviour recommended for many steel structures according to Table 3; and NZSP represents the NZS1170.5 (2019) pinched behaviour based on analyses to represent reinforced concrete behaviour according to Table 3. In part *f* of the figures, force-displacement response graphs are provided for the level of β considered to enable readers to see that the response has appropriate characteristics for that β. A summary of the trends with period, *T*, and loop shape factor, β, is given in Figure 10 for the extreme case when the ratcheting index, r_i, is 1.5, which is the maximum permitted without time history analyses according to NZS1170.5 (2016 and 2019).

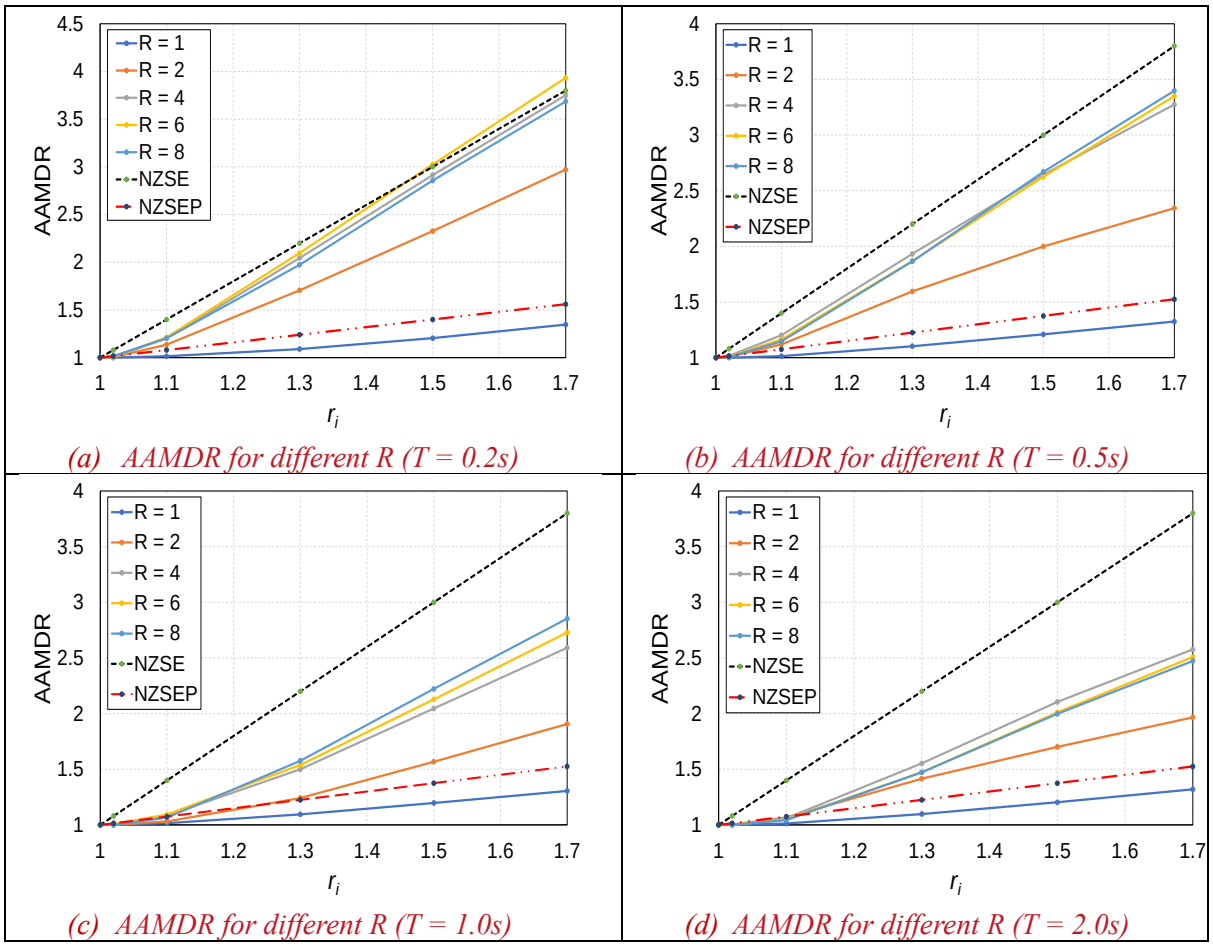

(a) AAMDR for different R (T = 0.2s)

(b) AAMDR for different R (T = 0.5s)

(c) AAMDR for different R (T = 1.0s)

(d) AAMDR for different R (T = 2.0s)

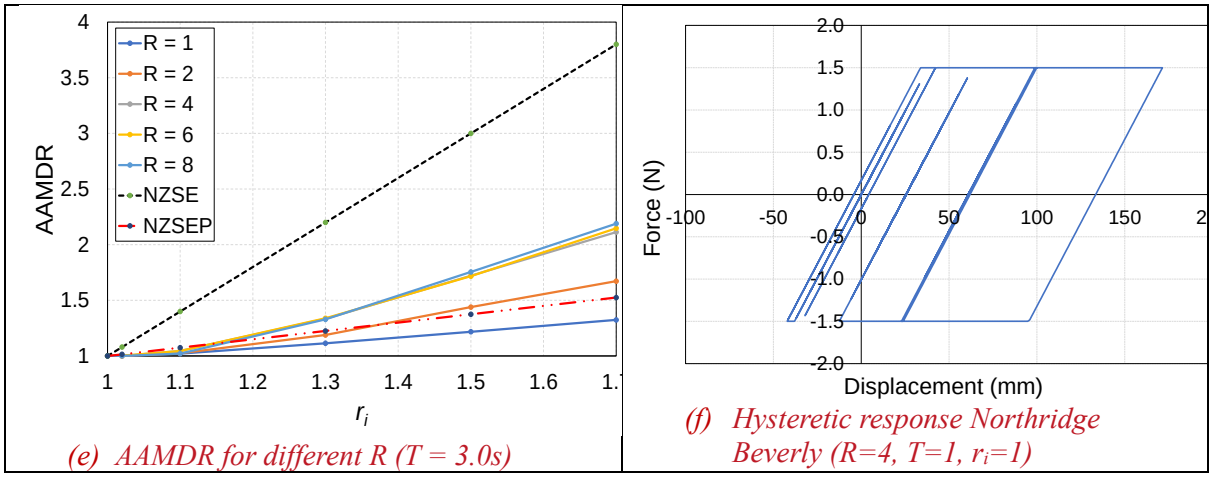

(e) AAMDR for different R (T = 3.0s)

(f) Hysteretic response Northridge Beverly (R=4, T=1, r_i=1)

Figure 5. Hysteretic response and average absolute maximum displacement ratio vs strength ratio for different period structure with β = 1, ξ = 5%, under FEMA P695 suite

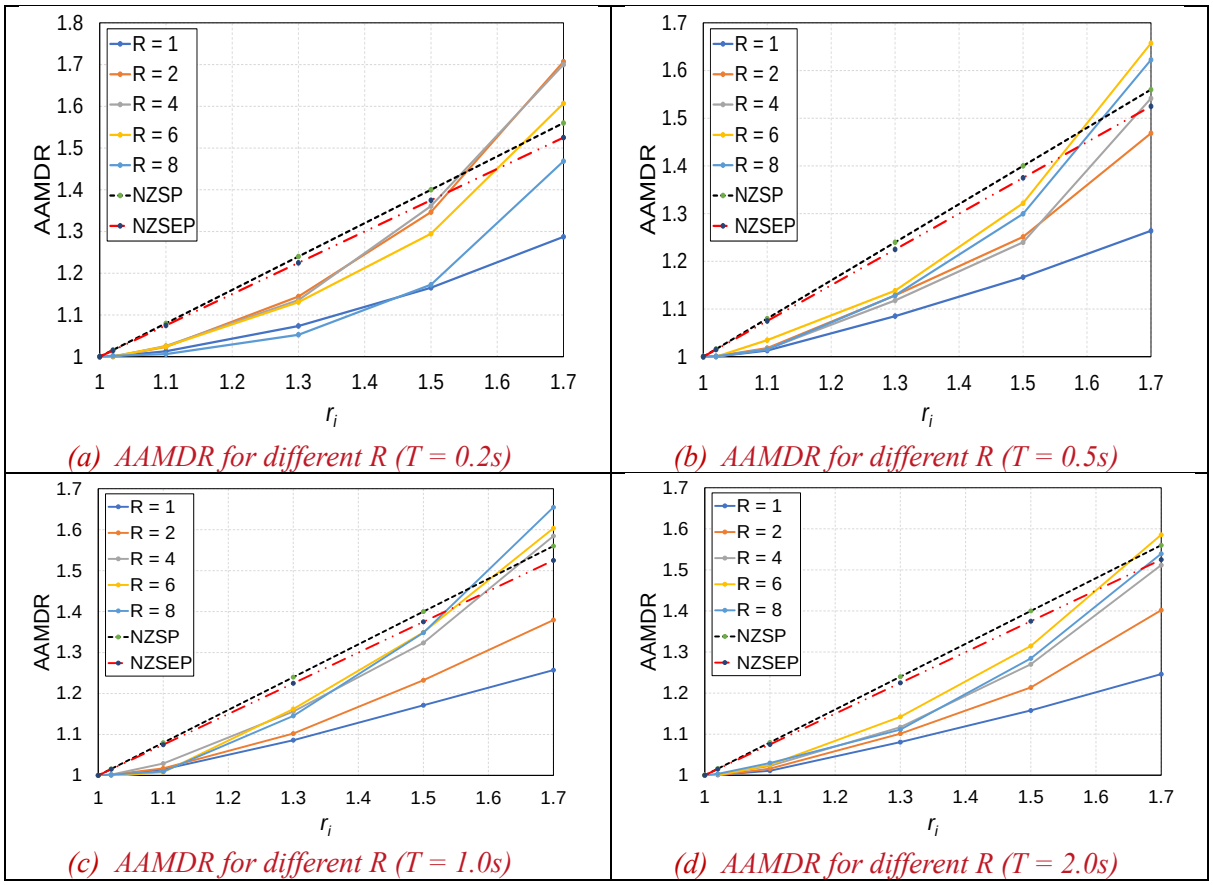

(a) AAMDR for different R (T = 0.2s)

(b) AAMDR for different R (T = 0.5s)

(c) AAMDR for different R (T = 1.0s)

(d) AAMDR for different R (T = 2.0s)

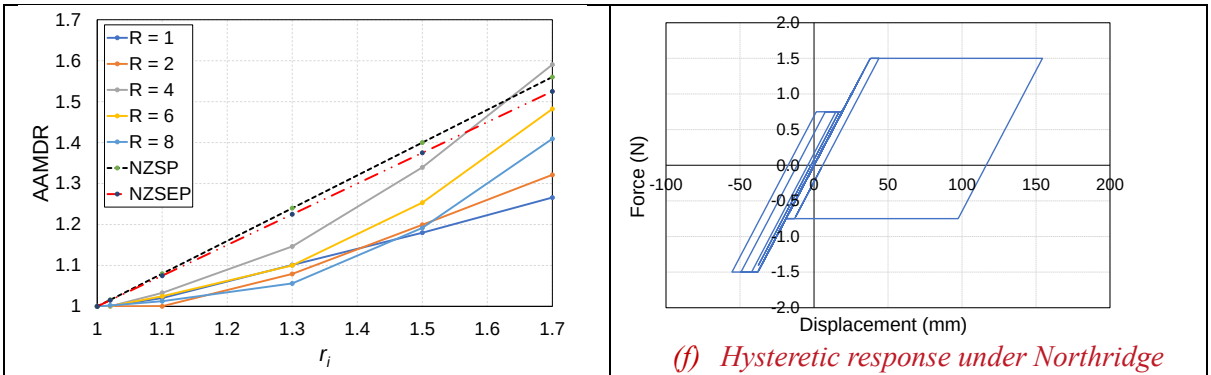

(e) AAMDR for different R (T = 3.0s)

(f) Hysteretic response under Northridge Beverly (R=4, T=1, r_i=1)

Figure 6. Average absolute maximum displacement ratio vs strength ratio for different period structure with β = 0.75, ξ = 5%, under FEMA P695 suite

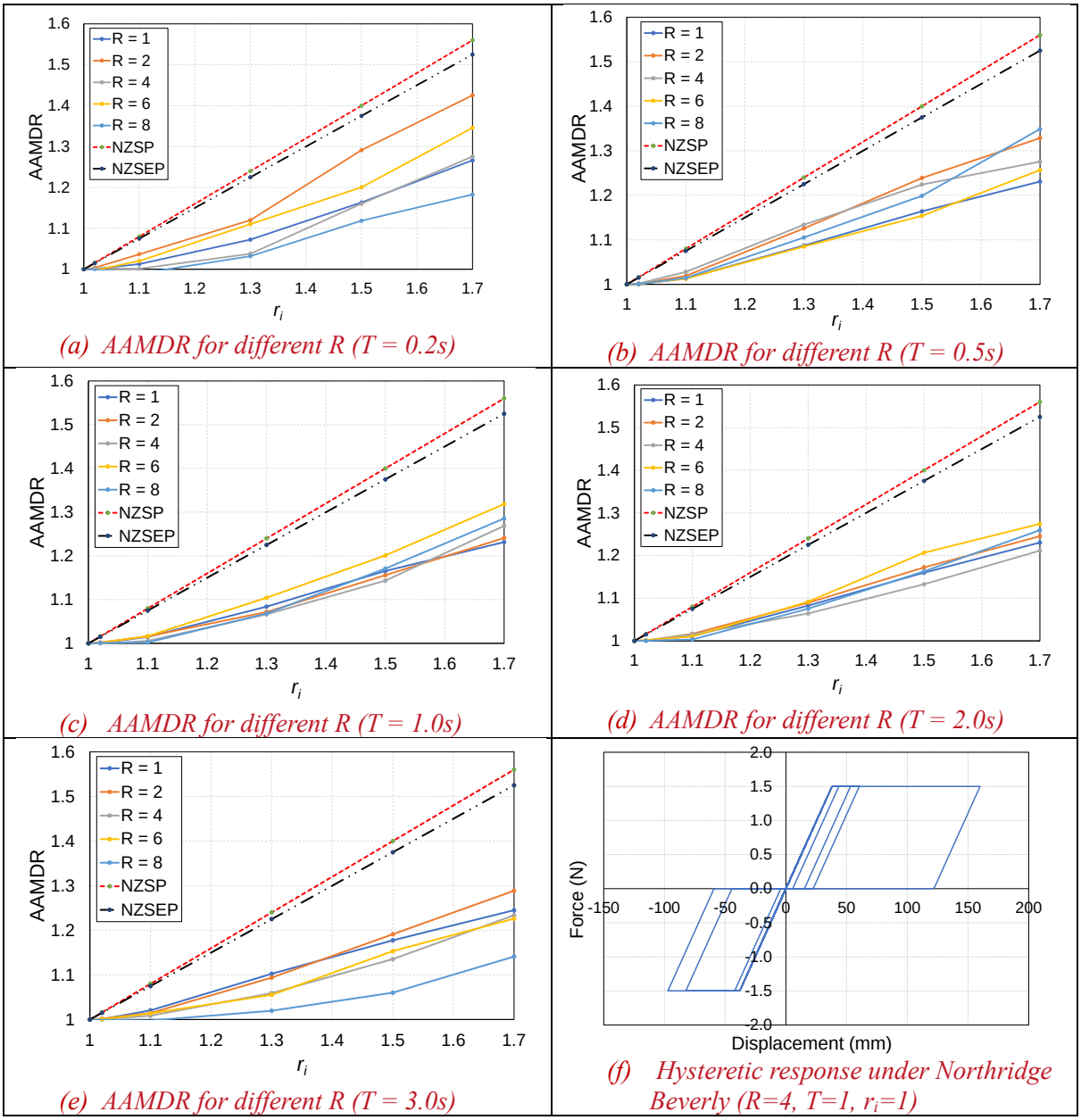

(a) AAMDR for different R (T = 0.2s)

(b) AAMDR for different R (T = 0.5s)

(c) AAMDR for different R (T = 1.0s)

(d) AAMDR for different R (T = 2.0s)

(e) AAMDR for different R (T = 3.0s)

(f) Hysteretic response under Northridge Beverly (R=4, T=1, r_i=1)

Figure 7. Average absolute maximum displacement ratio vs strength ratio for different period structure with β = 0.5, ξ = 5%, under FEMA P695 suite

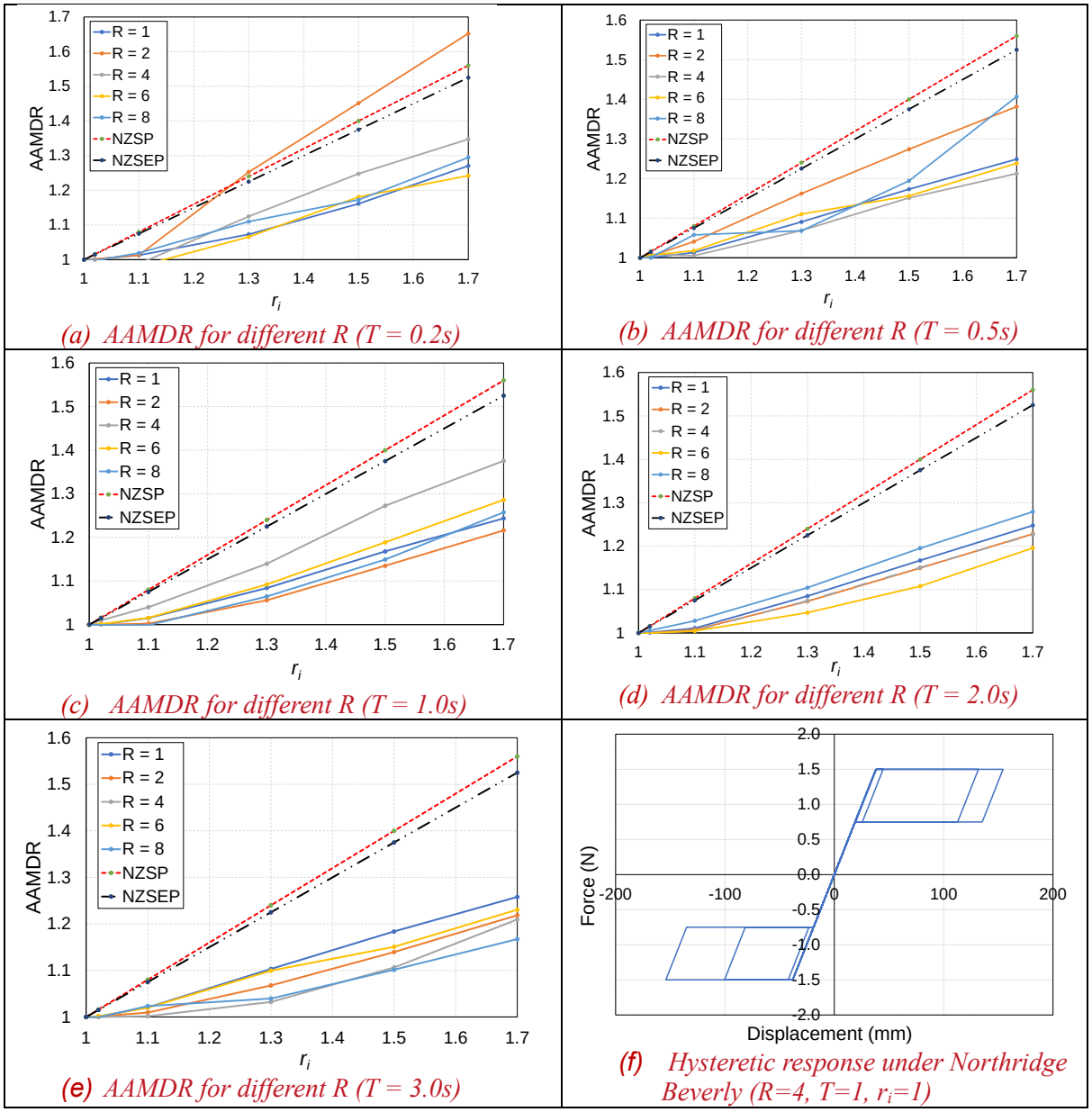

(a) AAMDR for different R (T = 0.2s)

(b) AAMDR for different R (T = 0.5s)

(c) AAMDR for different R (T = 1.0s)

(d) AAMDR for different R (T = 2.0s)

(e) AAMDR for different R (T = 3.0s)

(f) Hysteretic response under Northridge Beverly (R=4, T=1, r_i=1)

Figure 8. Average absolute maximum displacement ratio vs strength ratio for different period structure with β = 0.25, ξ = 5%, under FEMA P695 suite

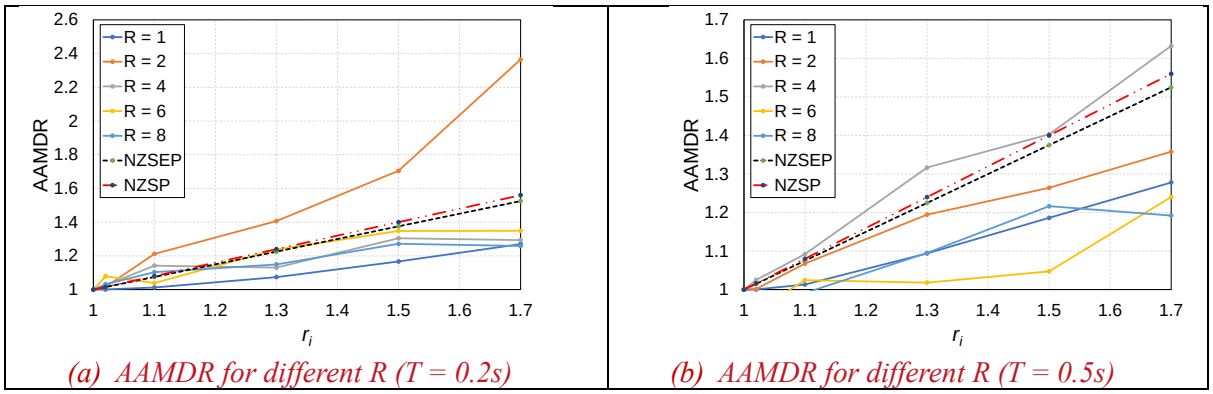

(a) AAMDR for different R (T = 0.2s)

(b) AAMDR for different R (T = 0.5s)

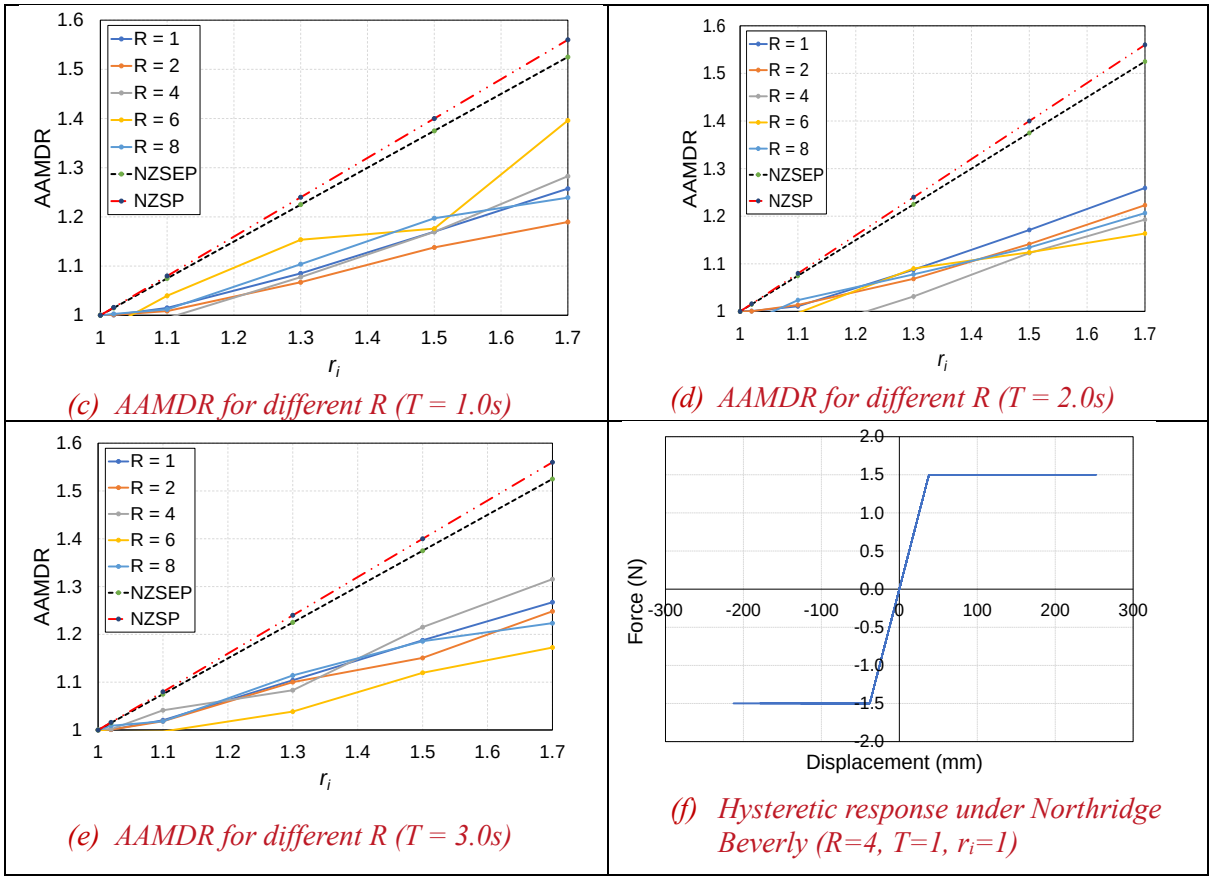

Figure 9. Average absolute maximum displacement ratio vs strength ratio for different period structure with β = 0, ξ = 5%, under FEMA P695 suite

Effect of r_i: In all figures AAMDR, which represents the displacement demand, increases with ratcheting index, r_i. This is because increasing strength difference in the two opposite directions causes the oscillator to yield more in the weaker direction compared to the stronger one.

Effect of R: For all structural periods, and β = 1, the AAMDR increases with higher *R* until *R* = 4. For higher values of *R*, such as 6 or 8, this trend stops. This relatively independence of AAMDR at high *R* is consistent with findings of Saif et al., (2017) and Dupuis et al., (2014) although the full reason for this is not known. For other β, there is more variation. For example, for β = 0.5, there is considerable variation with β for very short and very long periods, but for periods of 1.0-2.0s, the variation with *R* is small as shown in Figure 7.

Effect of T: As structural period increased, the ratchetting effect decreased. This is consistent with work by Farshbhaf et al. (2022) which indicates that structures with longer period are much more likely to be excited to larger displacements in the reverse direction because of fewer number of cycles in forward direction than structures with shorter periods in a ground motion record with a certain shaking duration. Because of this, it has fewer opportunities to ratchet.

Effect of β: The figures show that the AAMDR is higher for higher β. However, it was not sensitive with β when β was less than 1. It can be seen from Figure 10, there is a considerable reduction in ratcheting of oscillators when β was changed from 1 to 0.75. When β was less than 0.75 the change in AAMDR was low. The reduction of ratcheting tendency with β can be explained by the oscillation resistance ratio (ORR) concept described by Soleimankhani et al., (2021).

According to the ORR concept, oscillators with fatter hysteresis loops (e.g. β = 1) which have deformed to a certain displacement in one direction require more energy to reach the same maximum displacement in the reverse direction compared to the pinched hysteresis models because more input energy is

required from the ground motion. These β = 1 oscillators are therefore less likely to yield in the reverse direction and they are more likely to have residual displacement. This is likely to be in the weaker direction where they have the higher peak displacement according to the *hysteresis centre curve* (HCC) concept (MacRae and Kawashima, 1993). When shaking occurs again the structure is most likely to yield again in the weak direction according to the same considerations. The amount a structure with a certain design lateral force reduction factor, *R*, is likely to yield is related to the number of inelastic yielding events during the remainder of the record. A short period structure is likely to reach its strength more times than a longer period structure during a record of specific duration. Because of this, more ratcheting is expected in the shorter period structures with high β.

A structure with a lower β, is less susceptible to ratcheting because the structures tend to yield back toward their at-rest displacement position so the residual displacements before the next acceleration excursion are less. For the reason, the difference in AAMDR seen in Figure 10 is significantly affected by the loading curve, where the structure has less strength in one direction, than in the other. The unloading characteristic controls the structure velocity when it returns to the zero-force line but it may not be as important as the loading curve. Since the curves with different β all have the same loading characteristic, the AAMDR for pinched loops ($\beta \leq 0.75$) is similar in all cases averaging about 1.25 irrespective of period, *T*. The reason is independent of *T* is because, for a certain *R* and loading curve, it starts from a similar at-rest position, so there are no residual displacements, and the response for each inelastic excursion in a direction is therefore similar irrespective of whether the structure is subject to many (short *T*), for few (low *T*) cycles of deformation. This is different from fat (β = 1) oscillators where the combination of the residual displacements and the higher number of cycles mean that shorter period structures ratchet more.

4.2 Comparison with NZS1170.5 Ratcheting Recommendations

The NZS1170.5 (2019) recommendations given in Table 3 are categorized in two different sections based on the hysteretic behaviour of the structure under consideration. Two hysteretic behaviours mentioned in the NZS1170.5 (2019) requirements are the elastoplastic and the pinched hysteretic behaviours. Elastoplastic and pinched hysteretic loops may represent steel and reinforced concrete structures respectively.

Figure 5 presents AAMDR when the β = 1 and the post elastic stiffness was zero to obtain elastoplastic behaviour. It can be observed that the NZS1170.5 (2019) recommendations (NZSEP) generally conservatively estimate the steel structure AAMDR. However, the conservatism becomes high for higher period and for low *R*. Furthermore, NZS1170.5 (2016) (NZSE) which gives the same predictions for both steel and concrete structures, significantly underestimates the AAMDR for structures with high *R* and the full range of periods considered. This is consistent with Saif et al., (2022).

Accordingly, Figures 6, 7, 8, and 9 where the response of the oscillator is presented in terms of AAMDR for β = 0.75, 0.5, 0.25 and 0, respectively, with post elastic stiffness as zero, representing the range of pinched hysteretic behaviours to rocking behaviour that can be seen in Figure 6(f), 7(f), 8(f) and 9(f), respectively. The pinched hysteretic behaviour, possibly representing reinforced concrete (RC) structure response where those with a higher axial force generally have a more pinched (lower β) curve. Both the NZS1170.5 (2016) (NZSP) and NZS1170.5 (2019) (NZSEP) estimates for structures exhibiting pinched hysteretic behaviour, for AAMDR prediction are generally conservative (except for one case in Figure 9a where the analysis results were rechecked).

4.3 Design Considerations

The NZ1170.5 (2019) recommendations, also given by MacRae et al. (2022), for seismic ratcheting consideration generally provide a conservative estimation of displacement demands due to ratcheting for steel and reinforced concrete structures. However, simpler recommendations can be made for structures with $r_i \leq 1.5$, where the ratchetting is considered to be a function of the period, T, as shown in Figure 10 and in Equations 11 and 12. These curves, together with those from the NZ1170.5 (2019) recommendations, can be taken together as upper bounds on the AAMDR expected. In Equation 11, it is assumed that the elastoplastic hysteresis shape is that of the structure with the P-delta effect. It is noted that Equation 12 is more conservative than the value of 1.2 suggested by the Canadians in Table 1, possibly because they used a lower range of possible r_i.

$$AAMDR = 2.9 - 0.4T \quad \text{for structures with an elasto-plastic curve considering ductility} \quad (11)$$

$$AAMDR = 1.30 \quad \text{for pinched hysteretic structures} \quad (12)$$

Further work is required to refine the design recommendations based on considering all the parameters, and the range of structural forms used in practice.

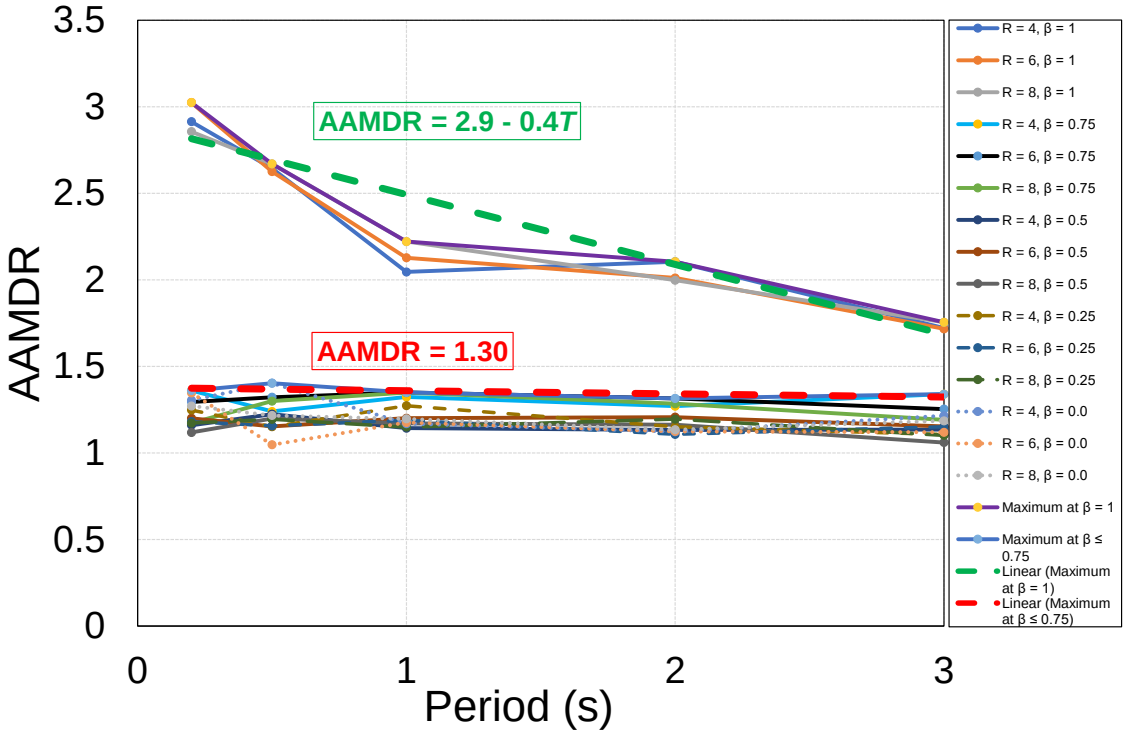

Figure 10. Average absolute maximum displacement ratio vs period of structure for different R and β, r_i = 1.5, ξ = 5% under FEMA P695 suite

5 CONCLUSION

This paper describes time history analyses conducted on a linear spring model with elastic-plastic flag-shaped hysteresis loops representing the range of structures with force-displacement hysteresis loops from non-linear elastic to elasto-plastic. It was found that:

1) The ratcheting tendency, represented by the average absolute maximum displacement ratio (AAMDR), tended to increase as the "ratio of the structural strengths on the forward (stronger) and reverse (weaker) directions", known as the ratcheting index, increased. For fatter (i.e. more elasto-plastic) hysteresis loops, the AAMDR was significantly greater than that of those with

pinched loops. It tended to increase with greater *R*, but generally converged so recommendations could be made independent of *R*. For elasto-plastic hysteresis loops, the AAMDR decreased with period, but for pinched loops it was small and independent of period.

2) Although generally conservative, the NZS1170.5 (2019) recommendations are sufficient to predict the ratcheting tendency of steel and concrete structures.
3) Simple prediction of the seismic ratcheting tendency of structures with a range of force-displacement hysteresis loops from non-linear elastic to elasto-plastic may be obtained (i) directly from the data, or (ii) by two simple equations which can be used together with the NZS1170.5 (2019) recommendations to provide an additional upper bound on the ratcheting displacements. These equations consider the effect of structural period and reduce the conservativism of the NZS1170.5 (2019) recommendations.

6 REFERENCES

Applied Technology Council (2009). "*FEMA P-695: Quantification of Building Seismic Performance Factors*". Federal Emergency Management Agency, Washington D.C, US.

Dupuis MR, Best TDD, Elwood KJ and Anderson DL (2014). "Seismic performance of shear wall buildings with gravity-induced lateral demands". *Canadian Journal of Civil Engineering*, **41**(4): 323-332. https://doi.org/10.1139/cjce-2012-0482

Cooper M, Fenwick R and Carter R (2012), "*The performance of Christchurch CBD Buildings Volume 2*". Canterbury Earthquake Royal Commission, Wellington, New Zealand. https://canterbury.royalcommission.govt.nz/Final-Report-Volume-Two-Contents

Japan Road Association (1990). "*Design Specifications for Highway Bridges, Part V: Seismic Design*". Japan Road Association, Tokyo, Japan.

Farshbaf M, Moghadam AS, MacRae GA, Lee C-L, Soleimankhani H, and Chang TL (2022). "Energy considerations for estimating displacements of oscillators with different hysteresis shapes". *New Zealand Society for Earthquake Engineering Annual Conference*. https://ir.canterbury.ac.nz/items/774d1951-5ef5-4956-8779-bf72fd0f46fe

Lee C-L (2019). "Efficient proportional damping model for simulating seismic response of large-scale structures". *7th International Conference on Computational Methods in Structural Dynamics and Earthquake Engineering (COMPDYN 2019)*, 4557–4564, 24-26 June, Athens. https://doi.org/10.7712/120119.7249.18776

Lee C-L (2020). "Proportional viscous damping model for matching damping ratios". *Engineering Structures*, **207** (3): 110178. https://doi.org/10.1016/j.engstruct.2020.110178

Lee C-L (2020). "Sparse proportional viscous damping model for structures with large number of degrees of freedom". *Journal of Sound and Vibration,* **478** (7): 115312. https://doi.org/10.1016/j.jsv.2020.115312

Lee C-L (2021). "Bell-shaped proportional viscous damping models with adjustable frequency bandwidth". *Computers & Structures*, **244** (2): 106423. https://doi.org/10.1016/j.compstruc.2020.106423

Lee C-L (2022). "Type 4 bell-shaped proportional damping model and energy dissipation for structures with inelastic and softening response". *Computers & Structures*, **258** (1): 106663. https://doi.org/10.1016/j.compstruc.2021.106663

Lee C-L and Chang TL (2023). "Implementation and performance of bell-shaped damping model". *In: Di Trapani, F., Demartino, C., Marano, G.C., Monti, G. (eds) Proceedings of the 2022 Eurasian OpenSees Days. EOS 2022. Lecture Notes in Civil Engineering*, vol **326**.Springer Cham. https://doi.org/10.1007/978-3-031-30125-4_13

MacRae GA and Kawashima K (1993). "The seismic response of bilinear oscillators using Japanese earthquake records". *Journal of Research*, Japan, **30**: 7-146. https://trid.trb.org/view/390457

MacRae GA, Lee C-L and Yeow TZ (2022). "Consideration for seismic ratcheting". *8th Asia Conference on Earthquake Engineering*, 9-11 November, Taipei, Taiwan. https://ir.canterbury.ac.nz/server/api/core/bitstreams/8ff3e73a-afd7-4062-b9fc-fd3c9adfbf7e/content

National Research Council (2015). "*National Building Code of Canada (NBCC)*". National Research Council of Canada, Ontario, Canada.

NZS1170.5 (2016). "NZS1170.5:2016 Structural Design Actions Part 5 Earthquake Actions", Standards New Zealand, Wellington, New Zealand.

Saif K, Lee C-L, Yeow TZ and MacRae GA (2018). "Seismic ratchetting of single-degree-of-freedom steel bridge columns". *Key Engineering Materials*, **763** (2): 295-300. https://doi.org/10.4028/www.scientific.net/kem.763.295

Saif K (2017). "*Seismic Ratcheting of RC Columns with Eccentric Gravity Loadings and Non-Symmetric Lateral Stiffness and Strength*". Master Thesis, Department of Civil and Natural Resources Engineering, University of Canterbury, Christchurch, New Zealand, 112. http://hdl.handle.net/10092/15051

Saif K, Lee C_L, MacRae GA, and Yeow TZ (2017). "Effect of eccentric moments on seismic ratcheting of single-degree-of-freedom structures". *New Zealand Society for Earthquake Engineering Annual Conference*, Wellington, New Zealand.

Saif, K., Yeow, T., Lee, C.-L., & MacRae, G. (2022). Interpretation and evaluation of NZS1170.5 2016 provisions for seismic ratcheting. Bulletin of the New Zealand Society for Earthquake Engineering, 55(3), 183–198. https://doi.org/10.5459/bnzsee.55.3.183-198.

Soleimankhani H, MacRae G and Sullivan T (2021). "The oscillation resistance ratio (ORR) for understanding inelastic response". *Bull. of the NZ Society for Earthquake Engineering,* **54** (4).

Yeow TZ, MacRae GA, Sadashiva VK and Kawashima K (2013). "Dynamic stability and design of c-bent columns". *J. of Earthquake Engineering*, **17** (5): 750–68. https://doi.org/10.1080/13632469.2013.771591

Yeow TZ and Kusunoki K (2023). "Seismic ratcheting of eccentric gravity loaded moment-resisting frame buildings". *Earthquake Engineering & Structural Dynamics,* **52** (4): 865–886. https://doi.org/10.1002/eqe.3790